JJEE
Volume 8, Number 3, September 2022
Pages 214-231
Jordan Journal of Electrical Engineering
ISSN (Print): 2409-9600, ISSN (Online): 2409-9619

New H-Infinity Tracking Control Algorithm in Linear Discrete-Time Systems

Seiichi Nakamori*

Emeritus Professor , Faculty of Education, Kagoshima University, Kagoshima, Japan
E-mail: k6165161@kadai.jp

Received: June 10, 2022 *Revised: July 04, 2022* *Accepted: July 12, 2022*

***Abstract*—** This paper proposes a new H-infinity quadratic tracking control (QTC) algorithm in linear discrete-time systems. This algorithm is a counterpart of the H-infinity QTC algorithm in linear continuous-time systems based on the integral equation approach. The discrete-time state equation in this paper has the control and exogenous inputs. Theorem 1 shows that the control and exogenous inputs in the H-infinity linear QTC problem are given by solving the two-point boundary value problem (TPBVP). Based on the TPBVP, Theorem 2 presents the H-infinity linear QTC algorithm for the control and exogenous inputs. The inputs use the information of two functions, which are calculated in the reverse direction of time from their terminal conditions. The control and exogenous inputs use the information of the state. The state observer uses the output of the system to estimate the state. A numerical simulation example shows the tracking control characteristics of the output estimate to the desired value and the characteristics of the estimates of the control and exogenous inputs. For the infinite value of the constant disturbance attenuation level γ, the proposed H-infinity linear QTC algorithm reduces to the linear QTC algorithm. The problem that can be solved for the minimum value of γ is the H-infinity linear QTC problem. For smaller value than the minimum value of γ, the H-infinity linear QTC algorithm diverges.

Keywords – H-infinity linear tracking control; Control input; Exogenous input; State observer; Discrete-time systems.

1. INTRODUCTION

In linear discrete-time systems, the control problems - such as the linear quadratic regulator (LQR) problem [1-3], the linear quadratic tracking control (QTC) problem [1, 4-8], the H-infinity LQR problem [9-11], and the H-infinity linear QTC problem [12-16] - have been extensively studied. The optimal tracking control algorithm is proposed using the reinforcement learning method in linear discrete-time systems [4]. The Q-learning algorithm of the infinite horizon linear quadratic tracker (LQT) computes the control input in terms of the learned kernel matrix without using full information on the system dynamics in discrete-time systems [5]. In [6], the optimal tracking control problem based on the reinforcement learning for linear discrete-time systems subject to multiple false data injection (FDI) attacks is considered. In [8], an iterative adaptive dynamic programming algorithm is proposed to solve the linear QTC problem without knowing the system dynamics. A value iteration technique is introduced to approximate the solution of the LQT Bellman optimality equation. The H-infinity linear tracking control algorithm in [12] is applicable to the state equation with a measurable reference signal term in addition to the control input and disturbance terms. In [13], the H-infinity linear preview control is applied to the servomechanism design. In the preview control, the future information of the reference signal or the disturbance is used. If the reference signal is constant, the disturbance in the augmented state equation becomes zero. In [14], the H-infinity linear tracking control algorithm is proposed for the observation equation with measurement noise. The H-infinity LQT simulation example in

* Corresponding author
Article's DOI: 10.5455/jjee.204-1654826074

[15] uses a discount factor of 0.98 for the value function. In [16], the discount factor in the disturbance attenuation condition is in the range (0,1). The discount factor for the value function in this paper is 1. The Q-learning-based H-infinity tracking control algorithm in [17] contains least-squares (LS) calculation. For linear continuous-time systems, the LQR and the H-infinity linear regulator are described [17, 18]. Based on an integral equation approach, the H-infinity linear QTC algorithm in continuous-time systems has been proposed [19]. Similar to the unified approach [19], this paper presents a new H-infinity linear QTC algorithm for discrete-time systems. In the H-infinity control problem [17, 18, 20], the system equation has the control input and the exogenous input (also called disturbance) in linear continuous-time systems. The discrete-time state equation in this paper has the control input and the exogenous input. Theorem 1 shows that the control and exogenous inputs in the H-infinity linear QTC problem are given by solving the two-point boundary value problem (TPBVP). Based on the TPBVP, Theorem 2 presents the H-infinity linear QTC control algorithm for the control and exogenous inputs. The inputs use the information of two functions, which are calculated in the reverse direction of time from their terminal conditions. The control and exogenous inputs use the information of the state. The state observer uses the output of the system to estimate the state. For the infinite value of the constant disturbance attenuation level, the proposed H-infinity linear QTC algorithm reduces to the linear QTC algorithm. The problem that can be solved for the minimum value of the constant disturbance attenuation level is the H-infinity tracking control problem. The H-infinity tracking control algorithm diverges for a smaller value than the minimum value of the constant disturbance attenuation level.

Two numerical simulation examples in section 4 show the characteristics for tracking the output estimate to the desired value and the properties of the control and exogenous input estimates. In the first example, the H-infinity linear QTC algorithm is compared with the existing H-infinity LQT [15]. The tracking accuracy of the H-infinity linear QTC algorithm in this paper is superior to that of the H-infinity LQT [15]. In the second example, the H-infinity linear QTC algorithm of Theorem 2 is applied to the simulation for the discrete-time F16 aircraft model.

2. H-INFINITY LINEAR QUADRATIC TRACKING CONTROL PROBLEM

Let the state equation for the state $x(k)$ and the output equation for the output $z(k)$ be given by:

$$\begin{aligned} &x(k+1) = Ax(k) + Gu(k), x(0) = c, \\ &G = [G_1 \quad G_2], u(k) = \begin{bmatrix} u_1(k) \\ u_2(k) \end{bmatrix}, \\ &z(k) = Cx(k), \end{aligned} \tag{1}$$

where $x(k) \in R^n$ is the state vector, $u(k) \in R^m$ is the input, and $z(k) \in R^l$ is the output. $u_1(k) \in R^{m_1}$ and $u_2(k) \in R^{m_2}$, $m_1 + m_2 = m$, are the control and exogenous inputs, respectively. Let us introduce $\|\tilde{z}(k)\|_2^2$ defined by Eq. (2). $\tilde{z}(k)$ is referred to as a performance output [20].

$$\|\tilde{z}(k)\|_2^2 = (\eta(k) - z(k))^T Q(k)\big(\eta(k) - z(k)\big) + u_1^T(k)\tilde{R}(k)u_1(k) \tag{2}$$

Here, $\eta(k)$ is the desired value. $Q(k)$ and $\tilde{R}(k)$ are positive definite matrices. We consider the finite-horizon H-infinity linear QTC problem. The task of H-infinity optimal linear QTC is to

find the control input $u_1(k)$ and exogenous input $u_2(k)$ based on the disturbance attenuation condition in Eq. (3) for the minimum value of γ. The problem of finding the minimum value of γ such that the H-infinity problem is solvable is called the H-infinity optimal problem. $\gamma > 0$ is the constant disturbance attenuation level, and as it is reduced, the control performance improves.

$$\sum_{k=0}^{L}(\eta(k)-z(k))^T Q(k)\big(\eta(k)-z(k)\big)+\sum_{k=0}^{L}u_1^T(k)\tilde{R}(k)u_1(k)\le\gamma^2\sum_{k=0}^{L}u_2^T(k)\,u_2(k) \tag{3}$$

The finite-horizon H-infinity linear QTC problem is equivalently transformed into a two-person zero-sum linear quadratic dynamic game [10, 16]. That is, given γ^2, we investigate the minimax problem to minimize the value function $\mathrm{J}(x,u_1,u_2)$ with respect to $u_1(k)$ and maximize $\mathrm{J}(x,u_1,u_2)$ with respect to $u_2(k)$.

$$\mathrm{J}(x,u_1,u_2)=\sum_{k=0}^{L}[(\eta(k)-z(k))^T Q(k)(\eta(k)-z(k))+u_1^T(k)\tilde{R}(k)u_1(k)-\gamma^2u_2^T(k)u_2(k)] \tag{4}$$

The worst-case disturbance $u_2(k)$ is the exogenous input, whereas $u_1(k)$ is the control input. Here, $Q(k)$ and $\tilde{R}(k)$ are symmetric positive definite matrices. Introducing $R(k)=\begin{bmatrix}\tilde{R}(k) & 0\\ 0 & -\gamma^2 I_{m_2\times m_2}\end{bmatrix}$, we can express Eq. (4) as follows.

$$J(x,u_1,u_2)=\sum_{k=0}^{L}[(\eta(k)-z(k))^T Q(k)(\eta(k)-z(k))+u^T(k)R(k)u(k)] \tag{5}$$

Eq. (5) represents the value function with the discount factor 1 for the H-infinity linear QTC problem in discrete-time systems. The state $x(k)$ is expressed as:

$$\begin{aligned}x(k)&=\Phi(k,0)c+\sum_{i=0}^{k-1}\Phi(k,i+1)Gu(i)\\&=\Phi(k,0)c+\sum_{i=0}^{L}1(k-i-1)\Phi(k,i+1)Gu(i)\,,\end{aligned} \tag{6}$$

$$1(\alpha)=\begin{cases}1, 0\le\alpha,\\ 0, \alpha<0,\end{cases}$$

$$\Phi(k,s)=\begin{cases}A^{k-s}, & 0\le s<k,\\ I, & k=s.\end{cases}$$

Here, $\Phi(k,s)$ is the state-transition matrix. $1(\alpha)$ represents the discrete-time unit step sequence. It should be noted that $\sum_{i=0}^{k-1}\Phi(k,i+1)Gu(i)=\sum_{i=0}^{L}1(k-i-1)\Phi(k,i+1)Gu(i)$ holds. Substituting Eq. (6) into Eq. (5), we get:

$$\begin{aligned}J(x,u_1,u_2)=\sum_{k=0}^{L}[&(\eta(k)-C\Phi(k,0)c\\&-C\sum_{k=0}^{L}1(k-i-1)\Phi(k,i+1)Gu(i))^T Q(k)(\eta(k)-C\Phi(k,0)c\\&-C\sum_{k=0}^{L}1(k-i-1)\Phi(k,i+1)Gu(i))+u(k)^T R(k)u(k)].\end{aligned} \tag{7}$$

To minimize the value function in Eq. (7) with respect to $u_1(k)$ and maximize Eq. (7) with respect to $u_2(k)$, we use the calculus of variations. Let $\breve{u}(k)$ be a vector with components of the optimal control input and the optimal exogenous input. Let ε be a scalar parameter with

extremely small positive value in the interval $0 \le k \le L$. Suppose $u(k)$ has a variant $\varepsilon\hat{\gamma}(k)$ from $\breve{u}(k)$ as:

$$u(k) = \breve{u}(k) + \varepsilon\hat{\gamma}(k). \tag{8}$$

We substitute Eq. (8) into Eq. (7). In the calculation of the variation $\Delta J = J(u(k)) - J(\breve{u}(k))$ for the value function, the ε term is the first variation and the ε^2 term is the second variation. Setting the first variation to 0 yields the necessary condition for the optimal $\breve{u}(k)$ as:

$$\begin{aligned} &R(k)\breve{u}(k) + \sum_{i=0}^{L}\sum_{j=0}^{L} 1(i-k-1)1(i-j-1)G^T\Phi^{\mathrm{T}}(i,k+1)C^TQ(i)C\Phi(i,j+1)G\breve{u}(j) \\ &= \textstyle\sum_{i=0}^{L} 1(i-k-1)G^T\Phi^T(i,k+1)C^TQ(i)(\eta(i) - C\Phi(i,0)c). \end{aligned} \tag{9}$$

Introducing

$$K(k,j) = \begin{cases} \displaystyle\sum_{i=k+1}^{L} G^T\Phi^T(i,k+1)C^TQ(i)C\Phi(i,j+1)\,, 0 \le j \le k \le L, \\ \displaystyle\sum_{i=j+1}^{L} G^T\Phi^T(i,k+1)C^TQ(i)C\Phi(i,j+1)\,, 0 \le k \le j \le L, \end{cases} \tag{10}$$

and

$$m(k+1) = -\sum_{i=k+1}^{L} G^T\Phi^T(i,k+1)C^TQ(i)\big(C\Phi(i,0)c - \eta(i)\big), \tag{11}$$

we obtain the equation for the optimal $\breve{u}(k)$ as:

$$R(k)\breve{u}(k) + \textstyle\sum_{j=0}^{L} K(k,j)G\breve{u}(j) = m(k+1). \tag{12}$$

The calculation that the second variation of ΔJ is positive yields $R(k)\delta_{k,s} + K(k,s)G > 0$. This inequality provides the sufficient condition for the value function $\mathrm{J}(x,u_1,u_2)$ to be optimal for control input $u_1(k)$ and exogenous input $u_2(k)$. Here, $\delta_{k,s}$ denotes the Kronecker delta function.

Similar to the unified approach in [19], Theorem 1 proposes from Eqs. (10) to (12) the TPBVP for the control input $u_1(k)$ and the exogenous input $u_2(k)$ in linear discrete-time systems. Theorem 2 proposes the new H-infinity linear QTC algorithm.

3. NEW H-INFINITY LINEAR QUADRATIC TRACKING CONTROL ALGORITHM AND STATE OBSERVER

Theorem 1 proposes the TPBVP for the control input $u_1(k)$ and the exogenous input $u_2(k)$.

Theorem 1: Let the state-space model be given by Eq. (1) in linear discrete-time systems. Eqs. (10) to (12) in section 2 is transformed into the TPBVP in Eqs. (13) and (14). In the H-infinity linear QTC, the control input $u_1(k)$ and the exogenous input $u_2(k)$ are represented by Eqs. (15) and (16), respectively. Here, $\eta(k)$ is the desired value.

$$\begin{aligned} &\alpha(k) = A^T\alpha(k+1) - C^TQ(k)(Cx(k) - \eta(k)), \\ &\text{Terminal condition: } \alpha(L+1) = 0 \end{aligned} \tag{13}$$

$$\begin{aligned} x(\mathrm{k}+1) &= Ax(k) + Gu(k), \\ &= Ax(k) + G_1u_1(k) + G_2u_2(k), \\ &\text{Initial condition: } x(0) = c \end{aligned} \tag{14}$$

Control input: $u_1(k)$

$$u_1(k) = \tilde{R}^{-1}(k)G_1^T\alpha(k+1) \tag{15}$$

Exogenous input: $u_2(k)$

$$u_2(k) = -\gamma^{-2}G_2^T\alpha(k+1) \tag{16}$$

Proof of Theorem 1 is deferred to Appendix A.

For $\gamma = \infty$ the H-infinity linear QTC problem reduces to the linear QTC problem in discrete-time systems. Hence, Eqs. (13) and (15) coincide with Eqs. (3) and (5) in [5], where $\alpha(k) = -\lambda(k)$.

The estimate $\hat{x}(k)$ of $x(k)$ is calculated by the state observer [21, 22]. The gain of the state observer is calculated with the pole placement method [21]. By using $\hat{x}(k)$ instead of $x(k)$, the estimates of $u_1(k)$ and $u_2(k)$ are denoted by $\hat{u}_1(k)$ and $\hat{u}_2(k)$, respectively. Apart from the state observer, the robust Chandrasekhar-type recursive least-squares Wiener filter is designed [23] in linear discrete-time stochastic systems.

Fig. 1 illustrates the structure of the H-infinity linear tracking controller and the state observer.

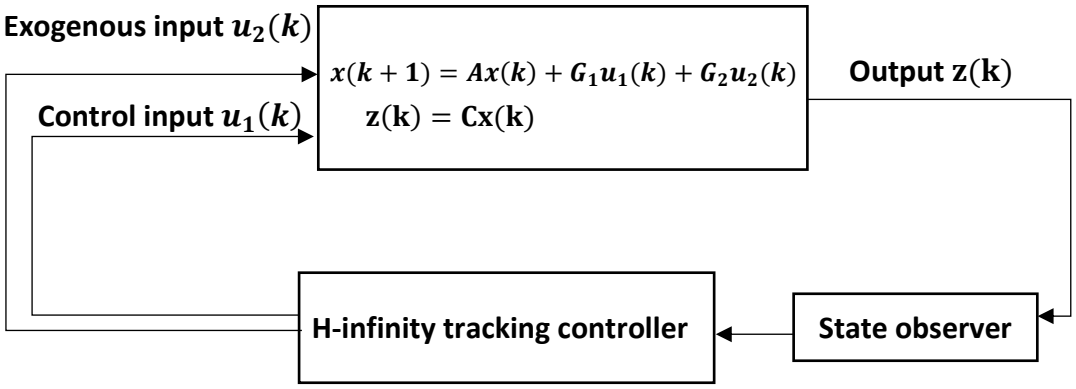

Fig. 1. Structure of H-infinity linear tracking controller and the state observer.

Theorem 2 proposes the new H-infinity linear QTC algorithm for the estimates of the control input $u_1(k)$ and the exogenous input $u_2(k)$ from the TPBVP in Theorem 1.

Theorem 2: Let $\eta(k)$ be the desired value and $R(k)$ be expressed by $R(k) = \begin{bmatrix} \tilde{R}(k) & 0 \\ 0 & -\gamma^2 I_{m_2\times m_2} \end{bmatrix}$. Let $u(k)$ has the components of the control input $u_1(k)$ and the exogenous input $u_2(k)$ as:

$$u(k) = \begin{bmatrix} u_1(k) \\ u_2(k) \end{bmatrix}, \tag{17}$$

then the estimate $\hat{u}(k)$ of $u(k)$ is calculated by Eqs. (18) to (22).

$$\hat{u}(k) = \begin{bmatrix} \hat{u}_1(k) \\ \hat{u}_2(k) \end{bmatrix}, \tag{18}$$

$$\begin{aligned} \hat{u}(k) = R^{-1}(k)G^T\{(A^T)^{-1}[A^{\mathrm{T}}P(k+1)(I - GR^{-1}(k)G^TP(k+1))^{-1}A + C^TQ(k)C] \\ - C^TQ(k)C\}\hat{x}(k) + R^{-1}(k)G^T(\mathrm{A}^T)^{-1}\{A^TP(k+1)(I \\ - GR^{-1}(k)G^TP(k+1))^{-1}GR^{-1}(k)G^T\xi(k+1) + \mathrm{A}^{\mathrm{T}}\xi(k+1) \\ - C^TQ(k)\eta(k)\} + R^{-1}(k)G^T(A^T)^{-1}C^TQ(k)\eta(k) \end{aligned} \tag{19}$$

$$\begin{aligned} &P(k) = A^TP(k+1)(\,I - GR^{-1}(k)G^TP(k+1))^{-1}A - C^TQ(k)C, \\ &\text{Terminal condition: } P(L+1) = 0 \end{aligned} \tag{20}$$

$$\xi(k) = A^T P(k+1)(I - GR^{-1}(k)G^T P(k+1))^{-1} GR^{-1}(k)G^T \xi(k+1) + A^T \xi(k+1) + C^T Q(k)\eta(k), \quad (21)$$

Terminal condition: $\xi(L+1) = 0$

In Eq. (19), $\hat{x}(k)$, the estimate of the state $x(k)$ computed by the discrete-time state observer [21], is used instead of $x(k)$. The state observer has the form:

$$\hat{x}(k+1) = A\hat{x}(k) + Gu(k) + K\big(z(k) - C\hat{x}(k)\big), \hat{x}(0) = 0, \quad (22)$$

where K is the observer gain. The observer gain is calculated using the pole placement method with $A - KC$ poles assigned [21]. $P(k)$ and $\xi(k)$ are computed from time $k = \mathrm{L} + 1$ in the reverse direction of time until steady-state values $\bar{P}$ and $\bar{\xi}$ are reached, respectively. The estimate $\hat{u}(k)$ of $u(k)$ is calculated by Eq. (19) using $\bar{P}$ and $\bar{\xi}$. In (19), $P(k+1)$ and $\xi(k+1)$ are replaced with their stationary values $\bar{P}$ and $\bar{\xi}$, respectively.

Proof of Theorem 2 is deferred to Appendix B. Fig. 2 shows the flowchart for the H-infinity linear QTC algorithm of Theorem 2.

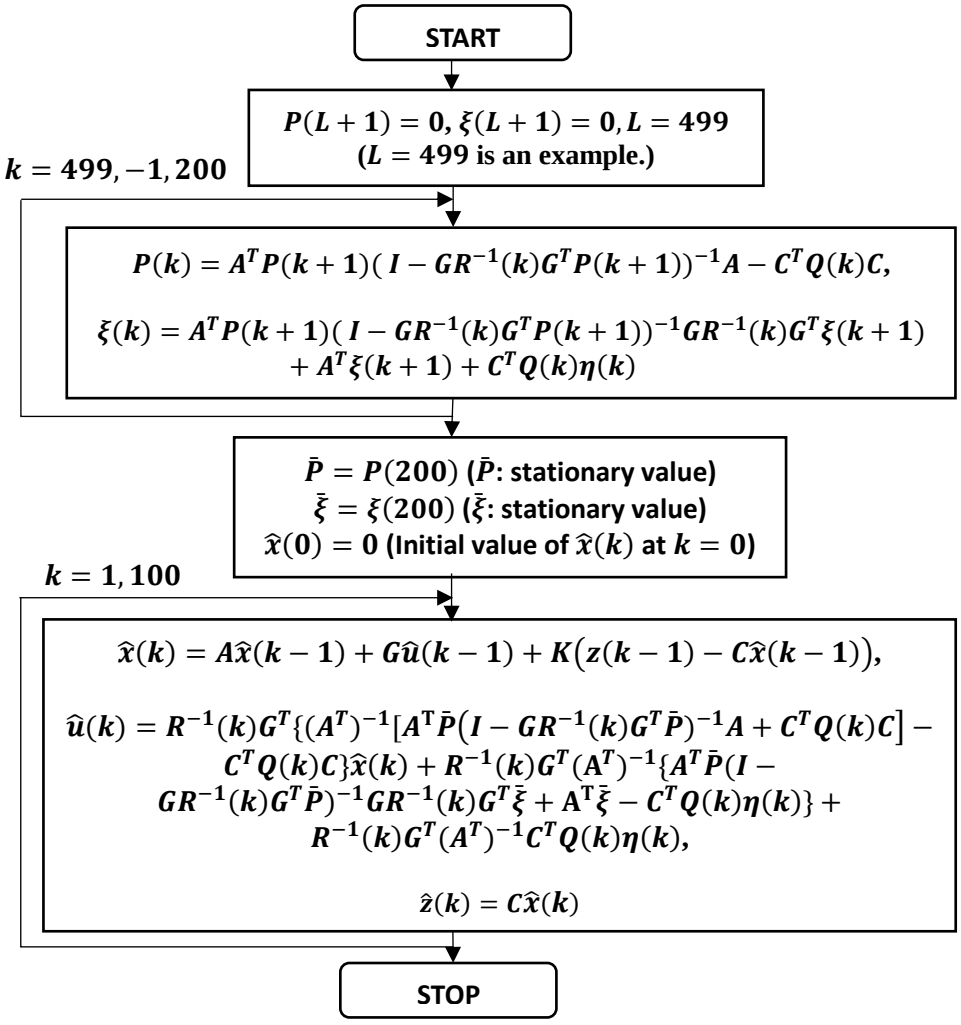

Fig. 2. Flowchart for H-infinity linear QTC algorithm of Theorem 2.

Section 4 presents two numerical simulation examples to show the characteristics of the proposed H-infinity linear QTC algorithm.

4. NUMERICAL SIMULATION EXAMPLES

EXAMPLE 1

Let the state equation for $x(k)$ and the output equation for $z(k)$ be given by:

$$\begin{bmatrix} x_1(k+1) \\ x_2(k+1) \end{bmatrix} = \begin{bmatrix} 0 & 1 \\ -0.4 & -1.3 \end{bmatrix} \begin{bmatrix} x_1(k) \\ x_2(k) \end{bmatrix} + \begin{bmatrix} 0 & 0 \\ 1 & 1 \end{bmatrix} \begin{bmatrix} u_1(k) \\ u_2(k) \end{bmatrix},$$
$$z(k) = [1 \quad 1] \begin{bmatrix} x_1(k) \\ x_2(k) \end{bmatrix}. \tag{23}$$

The system in Eq. (23) satisfies the controllability and observability conditions. It is worth noting that the exogenous input $u_2(k)$ is added to the control input $u_1(k)$. The estimate $\hat{x}(k) = \begin{bmatrix} \hat{x}_1(k) \\ \hat{x}_2(k) \end{bmatrix}$ of the state $x(k)$ and the estimate $\hat{u}(k) = \begin{bmatrix} \hat{u}_1(k) \\ \hat{u}_2(k) \end{bmatrix}$ of $u(k) = \begin{bmatrix} u_1(k) \\ u_2(k) \end{bmatrix}$ are calculated by substituting the system matrix $A = \begin{bmatrix} 0 & 1 \\ -0.4 & -1.3 \end{bmatrix}$, the input matrix $G = \begin{bmatrix} 0 & 0 \\ 1 & 1 \end{bmatrix}$, the observation vector $\mathrm{C} = [1 \quad 1]$, $R(k) = \begin{bmatrix} \tilde{R}(k) & 0 \\ 0 & -\gamma^2 \end{bmatrix}$, $Q(k) = 1$ and the desired value $\eta(k) = 10$ into the H-infinity linear QTC algorithm of Theorem 2. For the gain K, the eigenvalues of $A - KC$ in the state observer of Eq. (22) are set to 0.7 and 0.8. Since the poles of $A - KC$ are within the unit circle, $A - KC$ is a stable matrix. From the duality between control and estimation, the Octave commands "Po=[0.7 0.8]'", "pkg load control", and "K=place(A',C',Po)'" calculate the state observer gain as $K = \begin{bmatrix} -29.6 \\ 26.8 \end{bmatrix}$. The pole placement method is based on Ackermann's formula [21]. Fig. 3 illustrates the estimate $\hat{z}(k)$ of the output $z(k)$ vs. k for $R(k) = \begin{bmatrix} \tilde{R}(k) & 0 \\ 0 & -\gamma^2 \end{bmatrix}, \tilde{R}(k) = 0.0001, \gamma = 10$, by the H-infinity linear QTC algorithm of Theorem 2, and the H-infinity LQT [15] for $\gamma = 10$, $\tilde{R}(k) = 0.0001$, the discount factor 1 and $Q_x = \begin{bmatrix} I_{2\times2} & -I_{2\times2} \\ -I_{2\times2} & I_{2\times2} \end{bmatrix}$ in [15]. Here, Eqs. (23), (24) and (26) in [15] compute the control input and exogenous input. For $\gamma = 10$ the estimate $\hat{z}(k)$ by the H-infinity linear QTC algorithm of Theorem 2 tracks the desired value better than $\hat{z}(k)$ by the H-infinity LQT [15]. Table 1 shows the mean-square values (MSVs) of the output estimation errors $z(k) - \hat{z}(k)$ and the tracking errors $\eta(k) - \hat{z}(k)$, $1 \le k \le 1200$, by the H-infinity linear QTC algorithm of Theorem 2. Here, we compute $z(k) = C_{x(k)}$, $x(k+1) = Ax(k) + Gu(k)$, for $\gamma = 0.02$, $\gamma = 10$, and $\gamma = 100$ under the conditions $\tilde{R}(k) = 0.0001$ or $\tilde{R}(k) = 0.1$. In the computation of $u(k)$ with Eq. (19), $x(k)$ is used instead of the state observer estimate $\hat{x}(k)$. For each value of γ, the MSV of $z(k) - \hat{z}(k)$ is 0. This result indicates that the observer estimate $\hat{z}(k)$ coincides with $z(k)$. For $\tilde{R}(k) = 0.0001$, the MSVs of $\eta(k) - \hat{z}(k)$ are quite small for $\gamma = 0.02$, $\gamma = 10$, and $\gamma = 100$, indicating that the linear QTC algorithm of Theorem 2 has high tracking accuracy. In the case of $\tilde{R}(k) = 0.1$, the MSV of $\eta(k) - \hat{z}(k)$ for $\gamma = 0.02$ is considerably smaller than the MSV for $\gamma = 10$. It is seen that this is the effect of the H-infinity linear quadratic tracking controller. Table 2 shows the MSVs of tracking errors $\eta(k) - \hat{z}(k)$, $1 \le k \le 1200$, by the H-infinity LQT [15]. Here, we compute $z(k) = C_{x(k)}$, $\mathrm{x}(k+1) = Ax(k) + Gu(k)$, for $\gamma = 0.02$, $\gamma = 10$, and $\gamma = 100$ under the conditions $\tilde{R}(k) = 0.0001, R(k) = \begin{bmatrix} \tilde{R}(k) & 0 \\ 0 & -\gamma^2 \end{bmatrix}$, the discount factor $\lambda = 1$, and $Q_x = \begin{bmatrix} I_{2\times2} & -I_{2\times2} \\ -I_{2\times2} & I_{2\times2} \end{bmatrix}$ in [15]. $u(k)$ consists of the control input and the exogenous input, computed by Eqs. (23), (24) and (26) in [15]. The MSV

4.6548×10^{-6} by the H-infinity linear QTC algorithm of Theorem 2 for $\gamma = 100$, $\tilde{R}(k) = 0.0001$ is considerably smaller than the MSV 0.0211 by the H-infinity LQT [15] for $\gamma = 100$, $\tilde{R}(k) = 0.0001$. Thus, for $\gamma = 100$, $\tilde{R}(k) = 0.0001$, the tracking accuracy of the H-infinity LQT of Theorem 2 is superior to that of the H-infinity LQT [15] as well as for $\gamma = 10$, $\tilde{R}(k) = 0.0001$. The MSVs of $\eta(k) - \hat{z}(k)$ for $\gamma = 10$ and $\gamma = 100$ in the case of $\tilde{R}(k) = 0.0001$ by the H-infinity linear QTC algorithm of Theorem 2 have the same value 4.6548×10^{-6}. This indicates that the H-infinity linear QTC algorithm of Theorem 2 reduces to the linear QTC algorithm for larger γ values.

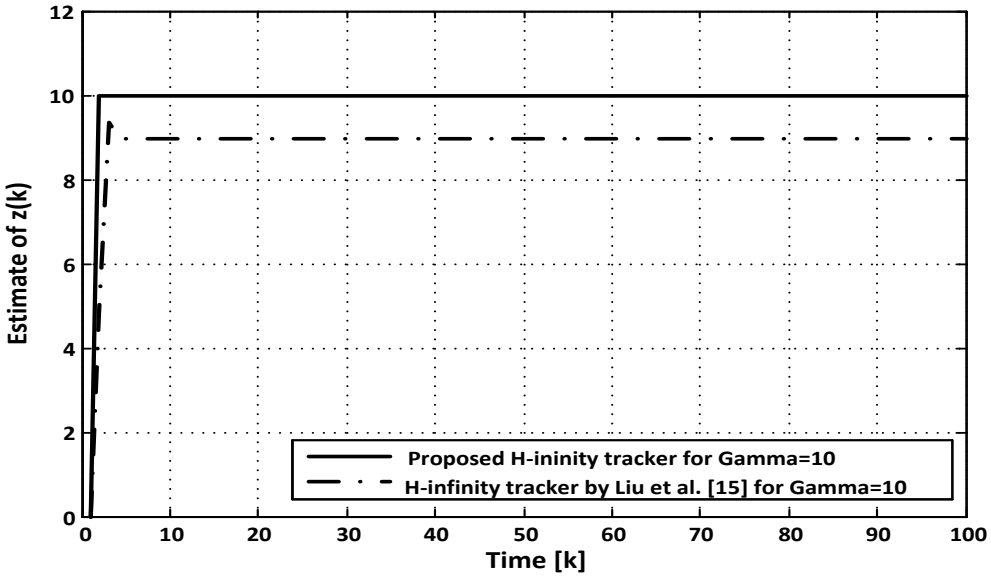

Fig. 3. Estimate $\hat{z}(k)$ of output $z(k)$ vs. k for $R(k) = \begin{bmatrix} \tilde{R}(k) & 0 \\ 0 & -\gamma^2 \end{bmatrix}, \tilde{R}(k) = 0.0001, \gamma = 10$ by H-infinity linear QTC algorithm of Theorem 2, and the H-infinity LQT [15] for $\tilde{R}(k) = 0.0001$, $\gamma = 10$, the discount factor 1, and $Q_x = \begin{bmatrix} I_{2\times2} & -I_{2\times2} \\ -I_{2\times2} & I_{2\times2} \end{bmatrix}$ in [15].

Table 1. Mean-square values of estimation errors $z(k) - \hat{z}(k)$ and tracking errors $\eta(k) - \hat{z}(k)$, $1 \le k \le 1200$, by H-infinity linear QTC algorithm of Theorem 2. $z(k) = C_{x(k)}$, $x(k+1) = Ax(k) + G\hat{u}(k)$.

	$\gamma = 0.02$		$\gamma = 10$		$\gamma = 100$	
	MSV of $z(k) - \hat{z}(k)$	MSV of $\eta(k) - \hat{z}(k)$	MSV of $z(k) - \hat{z}(k)$	MSV of $\eta(k) - \hat{z}(k)$	MSV of $z(k) - \hat{z}(k)$	MSV of $\eta(k) - \hat{z}(k)$
$\tilde{R}(k) = 0.0001$	0	7.9707×10^{-6}	0	4.6548×10^{-6}	0	4.6548×10^{-6}
$\tilde{R}(k) = 0.1$	0	4.6006×10^{-4}	0	2.3801	0	2.3761

Table 2. Mean-square values of tracking errors $\eta(k) - z(k)$, $1 \le k \le 1200$. $z(k) = C_{x(k)}$ by H-infinity LQT [15] for the discount factor $\lambda = 1$, and $Q_x = \begin{bmatrix} I_{2\times2} & -I_{2\times2} \\ -I_{2\times2} & I_{2\times2} \end{bmatrix}$ in [15].

	MSV of $\eta(k) - \hat{z}(k)$ for $\gamma = 0.02$	MSV of $\eta(k) - \hat{z}(k)$ for $\gamma = 10$	MSV of $\eta(k) - \hat{z}(k)$ for $\gamma = 100$
$\tilde{R}(k) = 0.0001$	divergence	1.0698	0.0211

Fig. 4 illustrates the estimate $\hat{u}_1(k)$ of the control input $u_1(k)$ vs. k for $R(k) = \begin{bmatrix} \tilde{R}(k) & 0 \\ 0 & -\gamma^2 \end{bmatrix}, \tilde{R}(k) = 0.0001, \gamma = 10$ by the H-infinity linear QTC algorithm of

Theorem 2. Fig. 5 illustrates the estimate $\hat{u}_2(k)$ of the exogenous input $u_2(k)$ vs. k for $R(k)=\begin{bmatrix}\tilde{R}(k) & 0\\ 0 & -\gamma^2\end{bmatrix}, \tilde{R}(k)=0.0001, \gamma=10$ by the H-infinity linear QTC algorithm of Theorem 2. Fig. 6 illustrates the estimate $\hat{z}(k)$ of the output $z(k)$ vs. k for $R(k)=\begin{bmatrix}\tilde{R}(k) & 0\\ 0 & -\gamma^2\end{bmatrix}, \tilde{R}(k)=0.0001, \gamma=0.02$ by the H-infinity linear QTC algorithm of Theorem 2. Fig. 7 illustrates the estimate $\hat{u}_1(k)$ of the control input $u_1(k)$ vs. k for $R(k)=\begin{bmatrix}\tilde{R}(k) & 0\\ 0 & -\gamma^2\end{bmatrix}, \tilde{R}(k)=0.0001, \gamma=0.02$ by the H-infinity linear QTC algorithm of Theorem 2. Fig. 8 illustrates the estimate $\hat{u}_2(k)$ of the exogenous input $u_2(k)$ vs. k for $R(k)=\begin{bmatrix}\tilde{R}(k) & 0\\ 0 & -\gamma^2\end{bmatrix}, \tilde{R}(k)=0.0001, \gamma=0.02$ by the H-infinity linear QTC algorithm of Theorem 2.

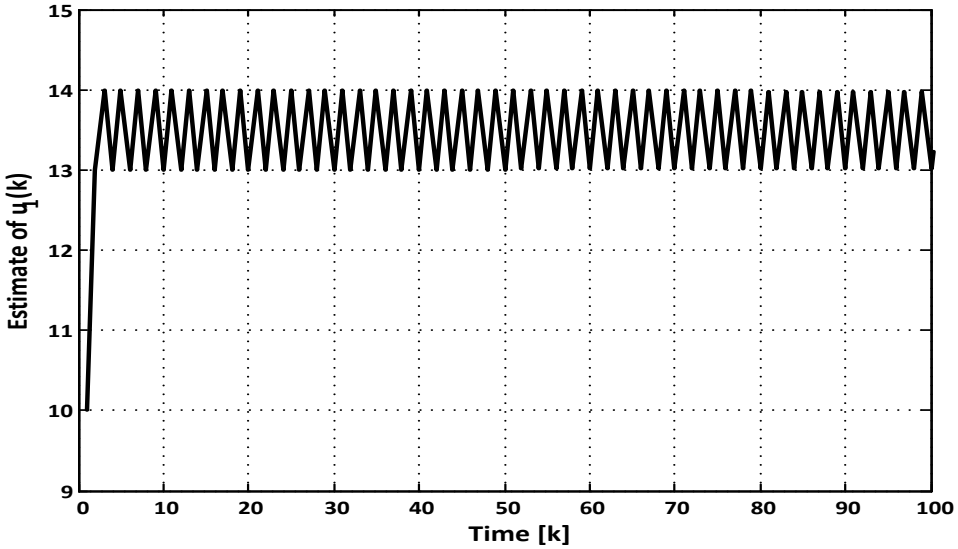

Fig. 4. Estimate $\hat{u}_1(k)$ of control input $u_1(k)$ vs. k for $R(k)=\begin{bmatrix}\tilde{R} & 0\\ 0 & -\gamma^2\end{bmatrix}, \tilde{R}(k)=0.0001, \gamma=10$ by H-infinity linear QTC algorithm of Theorem 2.

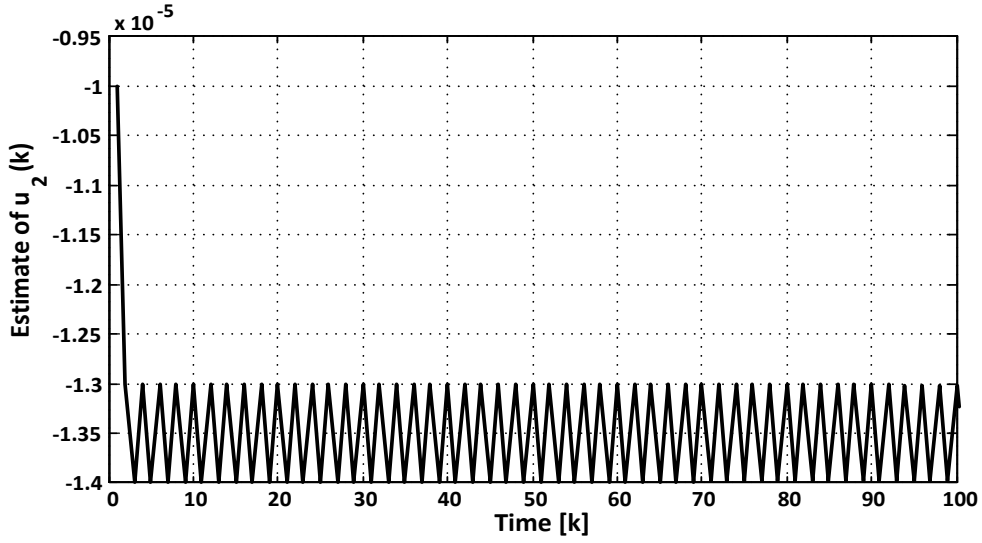

Fig. 5. Estimate $\hat{u}_2(k)$ of exogenous input $u_2(k)$ vs. k for $R(k)=\begin{bmatrix}\tilde{R}(k) & 0\\ 0 & -\gamma^2\end{bmatrix}, \tilde{R}(k)=0.0001, \gamma=10$ by H-infinity linear QTC algorithm of Theorem 2.

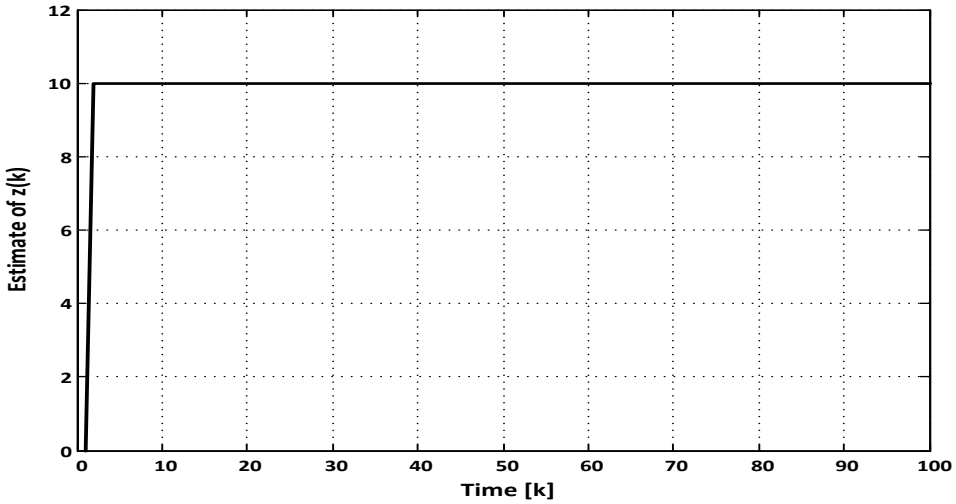

Fig. 6. Estimate $\hat{z}(k)$ of output $z(k)$ vs. k for $R(k) = \begin{bmatrix} \tilde{R}(k) & 0 \\ 0 & -\gamma^2 \end{bmatrix}, \tilde{R}(k) = 0.0001, \gamma = 0.02$ by H-infinity linear QTC algorithm of Theorem 2.

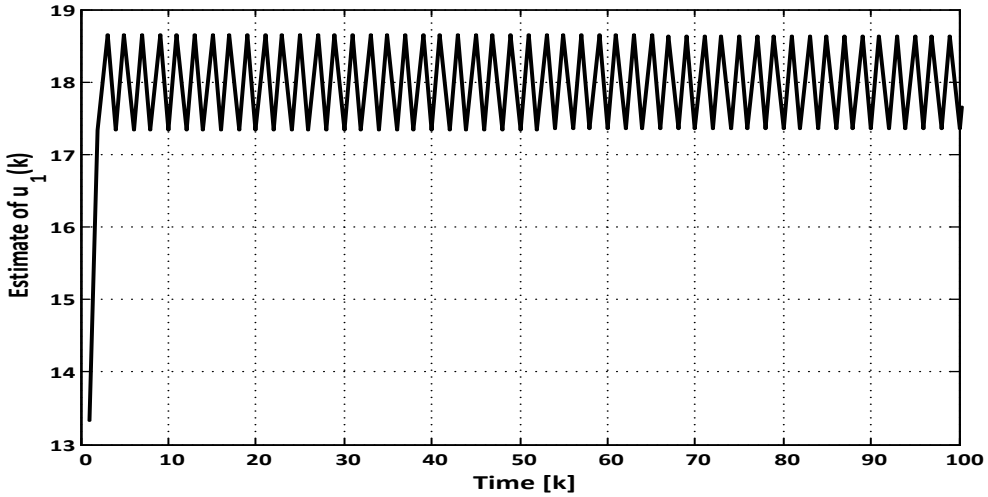

Fig. 7. Estimate $\hat{u}_1(k)$ of control input $u_1(k)$ vs. k for $R(k) = \begin{bmatrix} \tilde{R}(k) & 0 \\ 0 & -\gamma^2 \end{bmatrix}, \tilde{R}(k) = 0.0001, \gamma = 0.02$ by H-infinity linear QTC algorithm of Theorem 2.

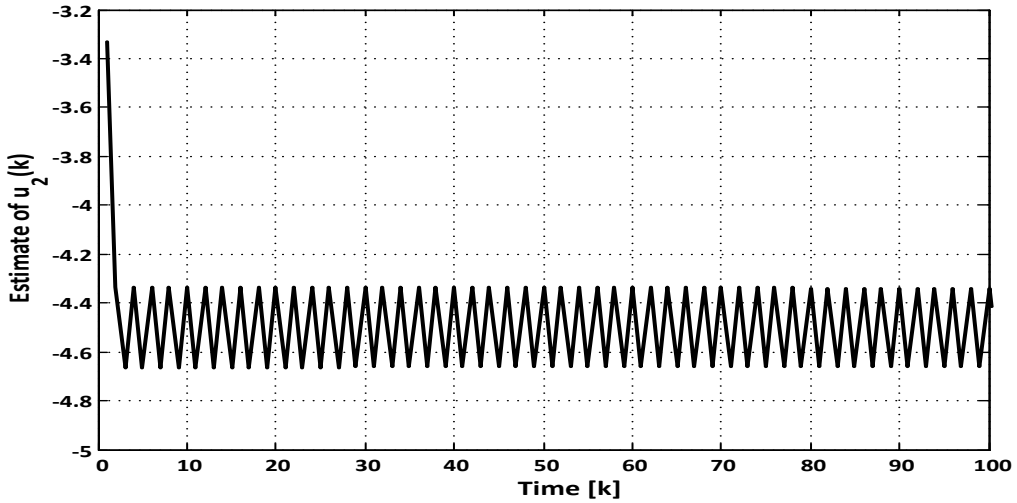

Fig. 8. Estimate $\hat{u}_2(k)$ of exogenous input $u_2(k)$ vs. k for $R(k) = \begin{bmatrix} \tilde{R}(k) & 0 \\ 0 & -\gamma^2 \end{bmatrix}, \tilde{R}(k) = 0.0001, \gamma = 0.02$ by H-infinity linear QTC algorithm of Theorem 2.

Figs. 3 and 6 show that, when $\tilde{R}(k) = 0.0001$, the output estimate $\hat{z}(k)$ waveforms by the H-infinity linear QTC algorithm of Theorem 2 are almost the same for $\gamma = 10$ and $\gamma = 0.02$.

Table 3 shows the mean values of $\hat{u}_1(k)$ and $\hat{u}_2(k)$, $1 \le k \le 1200$, under the conditions $\tilde{R}(k) = 0.0001$ or $\tilde{R}(k) = 0.1$ by the H-infinity linear QTC algorithm of Theorem 2. For $\gamma = 10$ and $\tilde{R}(k) = 0.0001$, the average absolute value of $\hat{u}_2(k)$ is found to be much smaller than for $\gamma = 0.02$ and $\tilde{R}(k) = 0.0001$, 1.3494×10^{-5} versus 4.4979. For $\gamma = 10$ and $\tilde{R}(k) = 0.0001$, the mean value of $\hat{u}_1(k)$ is smaller than for $\gamma = 0.02$ and $\tilde{R}(k) = 0.0001$, being 13.4944 versus 17.9914. For larger values of γ, such as $\gamma = 10$, the average absolute value of the exogenous input becomes so small that the exogenous input is almost negligible, and the H-infinity LQT is reduced to the LQT. From Eq. (3) this tendency can be understood by the relationship in Eq. (24). For the large value of γ, the denominator is small in comparison with the numerator.

$$\frac{\sum_{k=0}^{L}(\eta(k)-z(k))^T Q(k)\big(\eta(k)-z(k)\big)+\sum_{k=0}^{L}u_1^T(k)\tilde{R}(k)u_1(k)}{\sum_{k=0}^{L}u_2^T(k)\,u_2(k)} \le \gamma^2 \tag{24}$$

If γ is set to a small value, e.g., 0.01, the H infinity LQT diverges.

Table 3. Mean values of $\hat{u}_1(k)$ and $\hat{u}_2(k)$, $1 \le k \le 1200$, by H-infinity linear QTC algorithm of Theorem 2.

	$\gamma = 0.02$		$\gamma = 10$	
	Mean of $\hat{u}_1(k)$	Mean of $\hat{u}_2(k)$	Mean of $\hat{u}_1(k)$	Mean of $\hat{u}_2(k)$
$\tilde{R}(k) = 0.0001$	17.9914	-4.4979	13.4944	-1.3494×10^{-5}
$\tilde{R}(k) = 0.1$	-0.0542	13.5594	11.4262	-0.0114

EXAMPLE 2

In this simulation example, the H-infinity linear QTC algorithm of Theorem 2 is applied to the F16 aircraft discrete-time state-space model [9, 11] in (1) with

$$\begin{aligned} A &= \begin{bmatrix} 0.906488 & 0.0816012 & -0.0005 \\ 0.0741349 & 0.90121 & -0.0007083 \\ 0 & 0 & 0.132655 \end{bmatrix}, \\ G &= \begin{bmatrix} -0.00150808 & 0.00951892 \\ -0.0096 & 0.00038373 \\ 0.867345 & 0 \end{bmatrix}, \\ C &= [1 \quad 0 \quad 0]. \end{aligned} \tag{25}$$

The observer poles of $A - KC$ in this simulation example are set to 0.7, 0.8 and 0.6. The state $x(k) = \begin{bmatrix} \alpha(k) \\ q(k) \\ \delta_c(k) \end{bmatrix}$ has three components, i.e., the angle of attack $\alpha(k)$, the rate of pitch $q(k)$, and the elevator angle of deflection $\delta_c(k)$. The output $z(k)$ of the system is the angle of attack $\alpha(k)$. The desired value of $\alpha(k)$ is set to $\eta(k) = 0.1\ [rad]$. Let $Q(k) = 1$. Fig. 9 illustrates the estimate $\hat{z}(k)$ of the output $z(k)$ vs. k for $R(k) = \begin{bmatrix} \tilde{R}(k) & 0 \\ 0 & -\gamma^2 \end{bmatrix}, \tilde{R}(k) = 0.0001, \gamma = 0.1$. Fig. 10 illustrates the estimate $\hat{u}_1(k)$ of the control input $u_1(k)$ vs. k for $R(k) = \begin{bmatrix} \tilde{R}(k) & 0 \\ 0 & -\gamma^2 \end{bmatrix}, \tilde{R}(k) = 0.0001, \gamma = 0.1$. Fig. 11 illustrates the estimate $\hat{u}_2(k)$ of the exogenous input $u_2(k)$ vs. k for $R(k) = \begin{bmatrix} \tilde{R}(k) & 0 \\ 0 & -\gamma^2 \end{bmatrix}, \tilde{R}(k) = 0.0001, \gamma = 0.1$. Fig. 12 illustrates the estimate $\hat{z}(k)$ of the output

$z(k)$ vs. k for $R(k) = \begin{bmatrix} \tilde{R}(k) & 0 \\ 0 & -\gamma^2 \end{bmatrix}, \tilde{R}(k) = 0.0001, \gamma = 10$. Fig. 13 illustrates the estimate $\hat{u}_1(k)$ of the control input $u_1(k)$ vs. k for $R(k) = \begin{bmatrix} \tilde{R}(k) & 0 \\ 0 & -\gamma^2 \end{bmatrix}, \tilde{R}(k) = 0.0001, \gamma = 10$. Fig. 14 illustrates the estimate $\hat{u}_2(k)$ of the exogenous input $u_2(k)$ vs. k for $R(k) = \begin{bmatrix} \tilde{R}(k) & 0 \\ 0 & -\gamma^2 \end{bmatrix}, \tilde{R}(k) = 0.0001, \gamma = 10$. Rise time and overshoot of $\hat{z}(k)$ in Figs. 9 and 12 are almost the same. The waveforms of $\hat{u}_1(k)$ in Figs. 10 and 13 are almost the same. In comparison with the waveform of $\hat{u}_2(k)$ for $\gamma = 0.1$ in Fig. 11, the absolute value of $\hat{u}_2(k)$ for $\gamma = 10$ in Fig. 14 is considerably small in the stationary state.

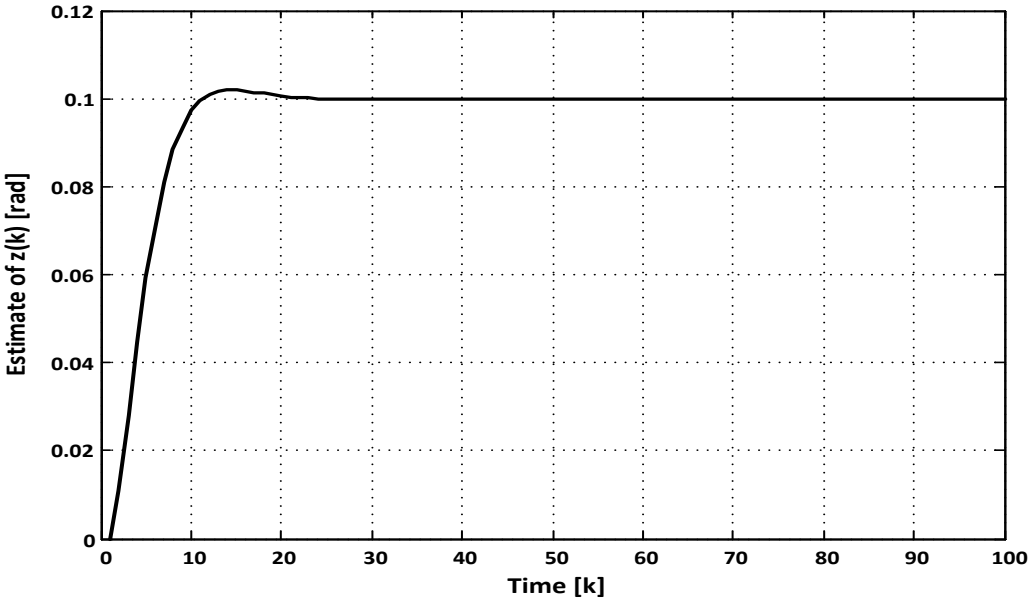

Fig. 9. Estimate $\hat{z}(k)$ of output $z(k)$ vs. k for $R(k) = \begin{bmatrix} \tilde{R}(k) & 0 \\ 0 & -\gamma^2 \end{bmatrix}, \tilde{R}(k) = 0.0001, \gamma = 0.1$.

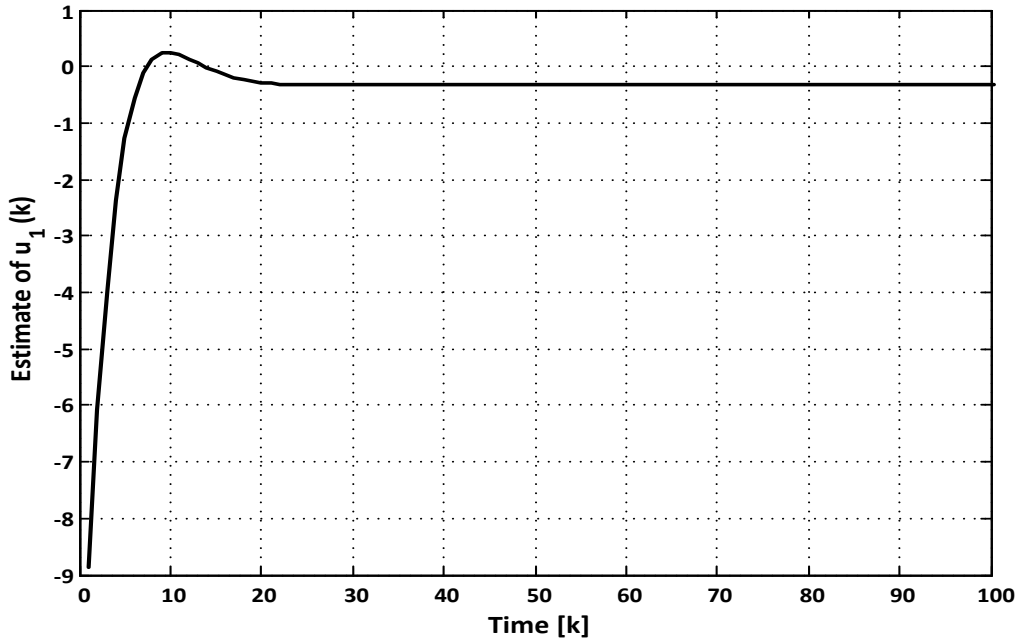

Fig. 10. Estimate $\hat{u}_1(k)$ of control input $u_1(k)$ vs. k for $R(k) = \begin{bmatrix} \tilde{R}(k) & 0 \\ 0 & -\gamma^2 \end{bmatrix}, \tilde{R}(k) = 0.0001, \gamma = 0.1$.

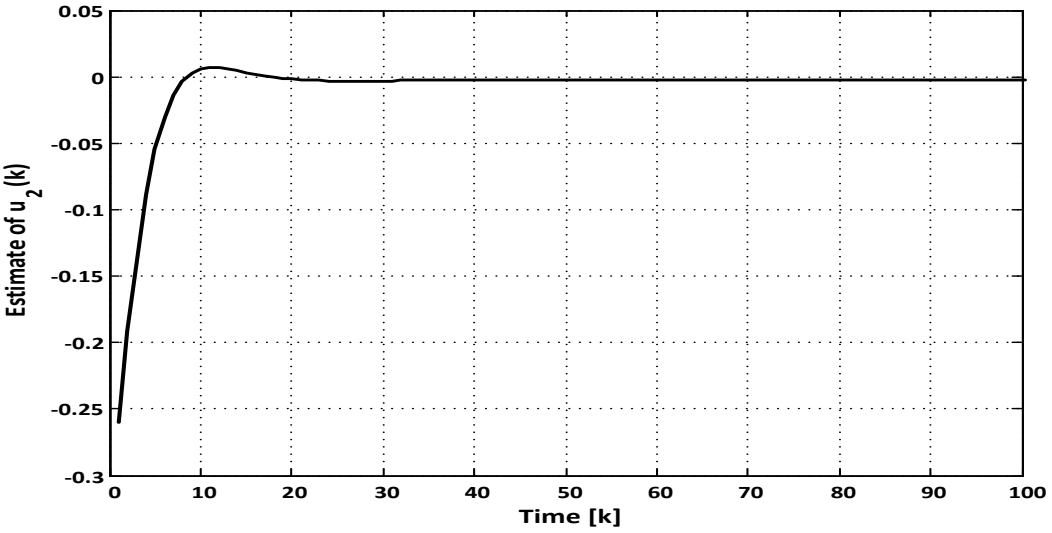

Fig. 11. Estimate $\hat{u}_2(k)$ of exogenous input $u_2(k)$ vs. k for $R(k) = \begin{bmatrix} \tilde{R}(k) & 0 \\ 0 & -\gamma^2 \end{bmatrix}, \tilde{R}(k) = 0.0001, \gamma = 0.1$.

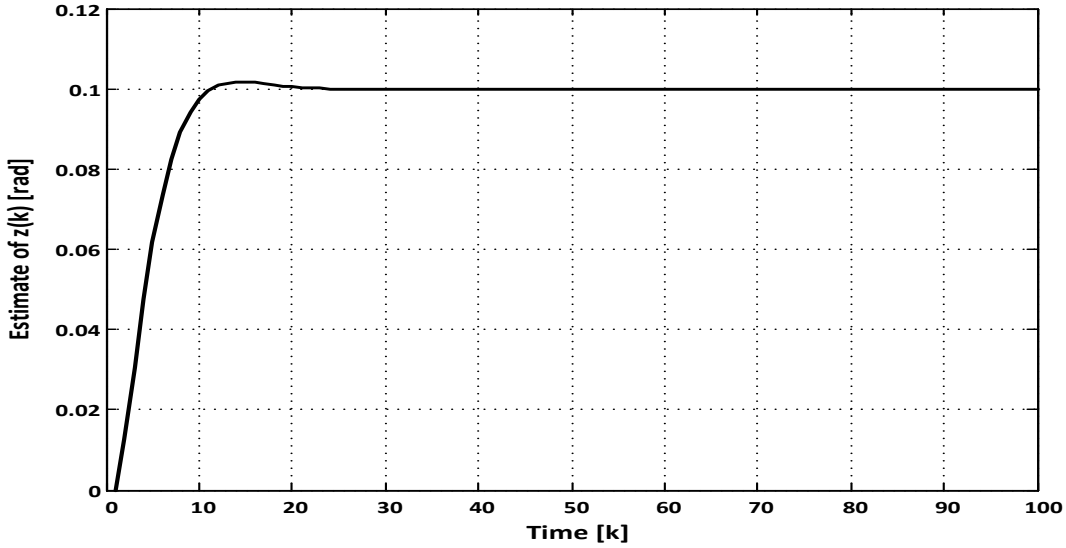

Fig. 12. Estimate $\hat{z}(k)$ of output $z(k)$ vs. k for $R(k) = \begin{bmatrix} \tilde{R}(k) & 0 \\ 0 & -\gamma^2 \end{bmatrix}, \tilde{R}(k) = 0.0001, \gamma = 10$.

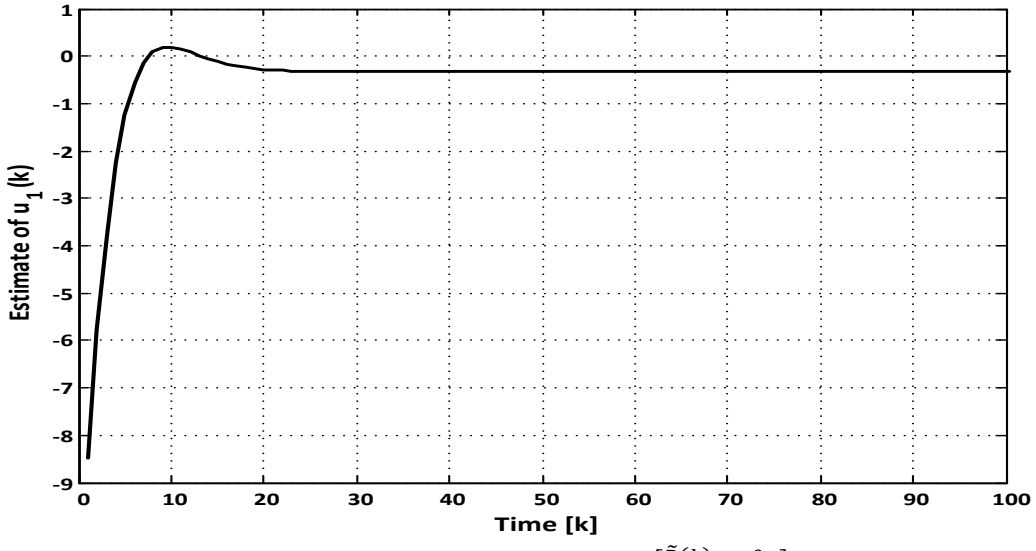

Fig. 13. Estimate $\hat{u}_1(k)$ of control input $u_1(k)$ vs. k for $R(k) = \begin{bmatrix} \tilde{R}(k) & 0 \\ 0 & -\gamma^2 \end{bmatrix}, \tilde{R}(k) = 0.0001, \gamma = 10$.

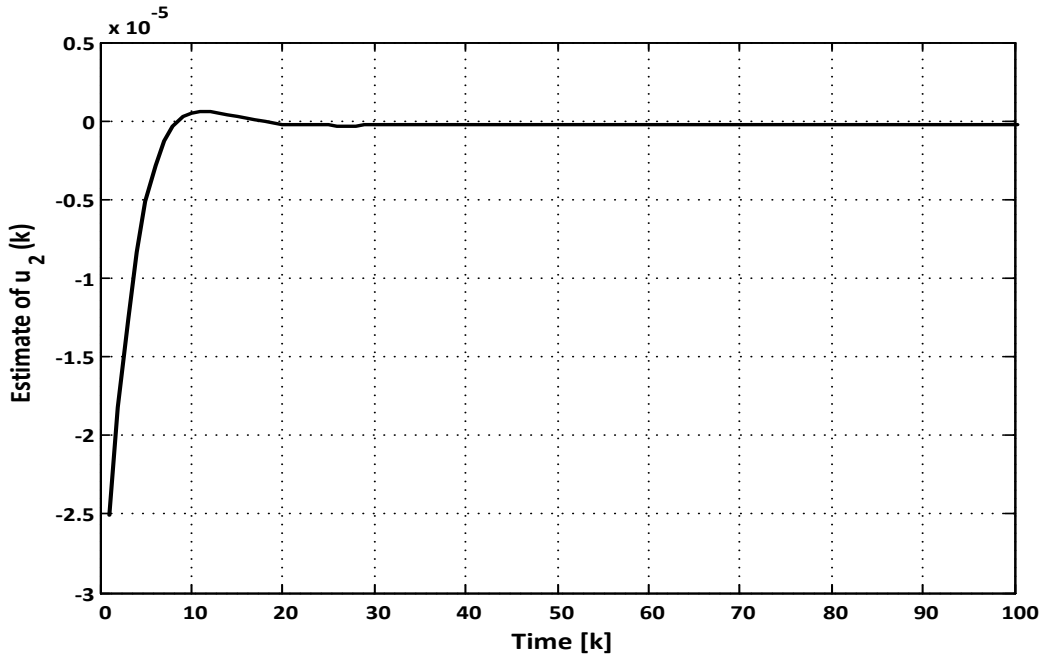

Fig. 14. Estimate $\hat{u}_2(k)$ of exogenous input $u_2(k)$ vs. k for $R(k) = \begin{bmatrix} \tilde{R}(k) & 0 \\ 0 & -\gamma^2 \end{bmatrix}, \tilde{R}(k) = 0.0001, \gamma = 10$.

Table 4 shows the MSVs of the estimation errors $z(k) - \hat{z}(k)$ and the tracking errors $\eta(k) - \hat{z}(k)$, $1 \le k \le 1200$. $z(k) = C_{x(k)}$, $\mathrm{x}(k+1) = Ax(k) + G\hat{u}(k)$, for $\gamma = 0.05$, $\gamma = 0.1$, $\gamma = 0.5$, and $\gamma = 10$ under the condition $\tilde{R}(k) = 0.0001$. For each value of γ, the MSV of $z(k) - \hat{z}(k)$ is zero, indicating that the observer estimate $\hat{z}(k)$ is equivalent to $z(k)$. The MSV of $\eta(k) - \hat{z}(k)$ is quite small for each value of γ. This result shows that the output estimate $\hat{z}(k)$ tracks the desired value $\eta(k)$ with high accuracy. Table 5 shows the mean values of $\hat{u}_1(k)$ and $\hat{u}_2(k)$, $1 \le k \le 1200$, under the condition $\tilde{R}(k) = 0.0001$. The mean values of $\hat{u}_1(k)$ for $\gamma = 0.05, \gamma = 0.1, \gamma = 0.5$, and $\gamma = 10$ are almost identical. For the mean values of $\hat{u}_2(k)$, as the value of γ increases, the absolute mean value of $\hat{u}_2(k)$ becomes small.

Table 4. Mean-square values of estimation errors $z(k) - \hat{z}(k)$ and tracking errors $\eta(k) - \hat{z}(k)$, $1 \le k \le 1200$. $z(k) = C_{x(k)}$, $\mathrm{x}(k+1) = Ax(k) + G\hat{u}(k)$

		MSV of $z(k) - \hat{z}(k)$	MSV of $\eta(k) - \hat{z}(k)$
$\tilde{R}(k) = 0.0001$	$\gamma = 0.05$	0	2.0585×10^{-5}
	$\gamma = 0.1$	0	1.6006×10^{-5}
	$\gamma = 0.5$	0	1.4914×10^{-5}
	$\gamma = 10$	0	1.4871×10^{-5}

Table 5. Mean values of $\hat{u}_1(k)$ and $\hat{u}_2(k)$, $1 \le k \le 1200$.

		Mean of $\hat{u}_1(k)$	Mean of $\hat{u}_2(k)$
$\tilde{R}(k) = 0.0001$	$\gamma = 0.05$	--0.3338	-0.0145
	$\gamma = 0.1$	-0.3204	-0.0035
	$\gamma = 0.5$	-0.3205	-1.3646×10^{-4}
	$\gamma = 10$	-0.3204	-3.4095×10^{-7}

5. CONCLUSIONS

This paper proposed a new H-infinity linear QTC algorithm in linear discrete-time systems. The presented algorithm is a counterpart to the H-infinity linear QTC algorithm in linear continuous-time systems based on the integral equation approach. As shown in section 2, setting the first variation of the value function to 0 provided the necessary condition for the optimal control and exogenous inputs. From the equations transformed from the necessary condition, Theorem 1 showed that the control and exogenous inputs in the H-infinity linear QTC problem are given by solving the TPBVP. Theorem 2 presented the H-infinity linear QTC algorithm for the control and exogenous inputs. The inputs used the information of the two functions, each computed in the reverse direction in time from the terminal conditions. The control and exogenous inputs used the information of the state. The state observer estimated the state with the output of the system. The inequality as the sufficient condition for the value function to be optimal for the control and exogenous inputs was also presented in section 2.

Two numerical simulation examples showed the tracking control characteristics of the proposed H-infinity linear QTC algorithm of Theorem 2. In the first example, when $\tilde{R}(k) = 0.0001$, the MSV of the tracking error showed that the H-infinity linear QTC algorithm of Theorem 2 is superior to the existing H-infinity LQT in tracking accuracy for $\gamma = 10$ and $\gamma = 100$, respectively. In the second example, when $\tilde{R}(k) = 0.0001$, the MSV of the tracking errors by the H-infinity linear QTC algorithm of Theorem 2 showed that it tracks the desired value with high accuracy for $\gamma = 0.05$, $\gamma = 0.1$, $\gamma = 0.5$, and $\gamma = 50$, respectively.

APPENDIX A: PROOF OF THEOREM 1

Introducing an $m \times m$ matrix $R(k)$ satisfying Eq. (A-1) and using Eqs. (10), (11), (A-2), and (A-3), Eq. (12) is rewritten as in Eq. (A-4).

$$R(k) = G^T B(k) G \tag{A-1}$$

$$\begin{aligned}\widetilde{K}(k,j) &= \begin{cases}\widetilde{K}_1(k,j), 0 \le j \le k \le L, \\ \widetilde{K}_2(k,j), 0 \le k \le j \le L\end{cases} \\ &= \begin{cases}\sum_{i=k+1}^{L} \Phi^T(i,k+1) C^T Q(i) C \Phi(i,j+1), 0 \le j \le k \le L, \\ \sum_{i=j+1}^{L} \Phi^T(i,k+1) C^T Q(i) C \Phi(i,j+1), 0 \le k \le j \le L\end{cases}\end{aligned} \tag{A-2}$$

$$\tilde{m}(k+1) = -\sum_{i=k+1}^{L} \Phi^T(i,k+1) C^T Q(i) \big(C\Phi(i,0)c - \eta(i)\big) \tag{A-3}$$

$$G^T\Big(B(k)Gu(k) + \sum_{j=0}^{k} \widetilde{K}_1(k,j)Gu(j) + \sum_{j=k+1}^{L} \widetilde{K}_2(k,j)Gu(j)\Big) = G^T \tilde{m}(k+1) \tag{A-4}$$

Here, the notations $\breve{u}$(k) and $\breve{u}$(j) in Eq. (12) are replaced with $u(k)$ and $u(j)$, respectively. The sufficient condition for Eq. (A-4) to hold is given by:

$$B(k)Gu(k) + \sum_{j=0}^{k} \widetilde{K}_1(k,j)Gu(j) + \sum_{j=k+1}^{L} \widetilde{K}_2(k,j)Gu(j) = \tilde{m}(k+1). \tag{A-5}$$

Introducing

$$\alpha(k+1) = B(k)Gu(k), \tag{A-6}$$

we have

$$\alpha(k+1)+\sum_{j=0}^{k}\widetilde{K}_1(k,j)Gu(j)+\sum_{j=k+1}^{L}\widetilde{K}_2(k,j)Gu(j)=\widetilde{m}(k+1). \tag{A-7}$$

Subtracting the equation obtained by putting $k \to k-1$ in Eq. (A-7) from Eq. (A-7) and noting $\widetilde{K}_1(k,k)Gu(k)-\widetilde{K}_2(k,k)Gu(k)=0$ from Eq. (A-2), we have:

$$\begin{aligned}\alpha(k+1)-\alpha(k)+\sum_{j=0}^{k-1}\left(\widetilde{K}_1(k,j)-\widetilde{K}_1(k-1,j)\right)Gu(j)\\ +\sum_{j=k}^{L}\left(\widetilde{K}_2(k,j)-\widetilde{K}_2(k-1,j)\right)Gu(j)=\widetilde{m}(k+1)-\widetilde{m}(k).\end{aligned} \tag{A-8}$$

From Eq. (A-2), we obtain Eqs. (A-9) and (A-10).

$$\begin{aligned}&\widetilde{K}_1(k,i)-\widetilde{K}_1(k-1,i)\\ &\quad=(I-\mathrm{A}^T)\sum_{j=k+1}^{L}\Phi^T(j,k+1)C^TQ(j)C\Phi(j,i+1)-C^TQ(k)C\Phi(k,i+1)\\ &\quad=(I-\mathrm{A}^T)\widetilde{K}_1(k,i)-C^TQ(k)C\Phi(k,i+1)\end{aligned} \tag{A-9}$$

$$\widetilde{K}_2(k,j)-\widetilde{K}_2(k-1,j)=(I-A^T)\,\widetilde{K}_2(k,j) \tag{A-10}$$

Substituting Eqs. (A-9) and (A-10) into Eq. (A-8), we have:

$$\begin{aligned}\alpha(k+1)-\alpha(k)+(I-\mathrm{A}^T)\sum_{j=0}^{L}\widetilde{K}(k,j)Gu(j)-C^TQ(k)C\sum_{j=0}^{k-1}\Phi(k,j+1)\,Gu(j)\\ =\widetilde{m}(k+1)-\widetilde{m}(k).\end{aligned} \tag{A-11}$$

From Eq. (A-3), we obtain the equation for $\widetilde{m}(k)$.

$$\widetilde{m}(k)=\mathrm{A}^T\widetilde{m}(k+1)-C^TQ(k)\big(C\Phi(k,0)c-\eta(k)\big) \tag{A-12}$$

From Eqs. (A-11), (A-12) and the relationship $x(k)=\Phi(k,0)c+\sum_{\mathrm{k}=0}^{\mathrm{k}-1}\Phi(k,i+1)Gu(i)$, after some manipulations, we get:

$$\alpha(k)=\mathrm{A}^T\alpha(k+1)-C^TQ(k)\big(Cx(k)-\eta(k)\big). \tag{A-13}$$

In Eq. (A-7), for $k=L$, from Eq. (A-2), $\widetilde{K}_1(L,j)$=0 and $\sum_{j=L+1}^{L}\widetilde{K}_2(L,j)Gu(j)=0$ are clear. Also, from Eq. (A-3), $\widetilde{m}(L+1)=0$ hods. Hence, $\alpha(L+1)=0$. From Eqs. (A-1) and (A-6), we have $u(k)=R^{-1}(k)G^T\alpha(k+1)$. According to $R=\begin{bmatrix}\tilde{R} & 0\\ 0 & -\gamma^2\end{bmatrix}$ and $u(k)=\begin{bmatrix}u_1(k)\\ u_2(k)\end{bmatrix}$ in Eq. (1), we obtain Eq. (15) for the control input $u_1(k)$ and Eq. (16) for the exogenous input $u_2(k)$.

APPENDIX B: PROOF OF THEOREM 2

Let $\alpha(k)$ be expressed by:

$$\alpha(k)=P(k)x(k)+\xi(k). \tag{B-1}$$

Substituting Eq. (B-1) into Eq. (13), we have:

$$P(k)x(k)+\xi(k)=\mathrm{A}^T(P(k+1)x(k+1)+\xi(k+1))-C^TQ(k)(Cx(k)-\eta(k)). \tag{B-2}$$

From $u(k)=R^{-1}(k)G^T\alpha(k+1)$ and Eq. (B-1), we have:

$$\begin{aligned}x(k+1)&=Ax(k)+Gu(k)\\ &=Ax(k)+GR^{-1}(k)G^T\alpha(k+1)\\ &=Ax(k)+GR^{-1}(k)G^T(P(k+1)x(k+1)+\xi(k+1)).\end{aligned} \tag{B-3}$$

From Eq. (B-3), $x(k+1)$ is expressed as:

$$x(k+1)=(I-GR^{-1}(k)G^TP(k+1))^{-1}(Ax(k)+GR^{-1}(k)G^T\xi(k+1)). \tag{B-4}$$

Substituting Eq. (B-4) into Eq. (B-2) and equating the $x(k)$ terms on the left and right sides,

we obtain Eq. (20) for $P(k)$. In this case, the terms on the left and right sides, except for the $x(k)$ term, are equal, so we obtain Eq. (21) for $\xi(k)$. Since $\alpha(L+1)=0$ in Eq. (13), we set $P(L+1)=0$ and $\xi(L+1)=0$ from Eq. (B-1).

REFERENCES

[1] F. Lewis, D. Vrabie, V. Syrmos, *Optimal Control*, 3rd Edition, John Wiley and Sons, 2012.

[2] J. Zhao, C. Zhang, "Finite-horizon optimal control of discrete-time linear systems with completely unknown dynamics using Q-learning," *Journal of Industrial and Management Optimization*, vol. 17, no. 3, pp. 1471–1483, 2021.

[3] Q. Zhao, H. Xu, J. Sarangapani, "Finite-horizon near optimal adaptive control of uncertain linear discrete-time systems," *Optimal Control Applications Methods*, vol. 36, no. 6, pp. 853–872, 2015.

[4] B. Kiumarsi, F. Lewis, M. Naghibi-Sistani, A. Karimpour, "Optimal tracking control for linear discrete-time systems using reinforcement learning," in *52nd IEEE Conference on Decision and Control*, pp. 3845–3850, 2013.

[5] B. Kiumarsi, F. Lewis, H. Modares, A. Karimpour, M. Sistani, "Reinforcement Q-learning for optimal tracking control of linear discrete-time systems with unknown dynamics," *Automatica*, vol. 50, no. 4, pp. 1167-1175, 2014.

[6] H. Liu, H. Qiu, "Optimal tracking control of linear discrete-time systems under cyber attacks," *IFAC PapersOnLine*, vol. 53, no. 2, pp. 3545-3550, 2020.

[7] K. Baharea, L. Frank, N. Mohammad-Bagherb, K. Alib, "Optimal tracking control of unknown discrete-time linear systems using input-output measured data," *IEEE Transactions on Cybernetics*, vol. 45, no. 12, pp. 2770–2779, 2015.

[8] X. Li, L. Xue, C. Sun, "Linear quadratic tracking control of unknown discrete-time systems using value iteration algorithm," *Neurocomputing*, vol. 314, pp. 86–93, 2018.

[9] S. Rizvi, Z. Lin, "Output feedback Q-learning for discrete-time linear zero-sum games with application to the H-infinity control," *Automatica*, vol. 95, pp. 213–221, 2018.

[10] X. Li, L. Xi, W. Zha, and Z. Peng, "Minimax Q-learning design for H∞ control of linear discrete-time systems," *Frontiers of Information Technology and Electronic Engineering*, vol. 23, pp. 438–451, 2022.

[11] A. Al-Tamimi, F. Lewis, M. Abu-Khalaf, "Model-free Q-learning designs for linear discrete-time zero-sum games with application to H-infinity control," *Automatica*, vol. 43, pp. 473–481, 2007.

[12] L. Xie, M. Fu, C. E. de Souza, "H_∞ control and quadratic stabilization of systems with parameter uncertainty via output feedback," *IEEE Transactions on Automatic Control*, vol. 37, no. 8, pp. 1253–1256, 1992.

[13] K. Takaba, "A tutorial on preview control systems," *SICE Annual Conference in Fukui*, Fukui, Japan, vol. 2, pp. 1561–1566, 2003.

[14] P. Rawicz, P. Kalata, K. Murphy, T. Chmielewski, "Discrete time H_∞ control/estimation applied to the target tracking problem using a variation of parameters approach," in *Proceedings of the 2000 American Control Conference*, vol. 2, pp. 1298–1302, 2000.

[15] Y. Liu, Z. Wang, Z. Shi, "H∞ tracking control for linear discrete-time systems via reinforcement learning," *International Journal of Robust and Nonlinear Control*, vol. 30, no. 1, pp. 282–301, 2020.

[16] Y. Yang, Y. Wan, J. Zhu, F. L. Lewis, "H∞ tracking control for linear discrete-time systems: model-free Q-learning designs," *IEEE Control Systems Letters*, vol. 5, no. 1, pp. 175–180, 2021.

[17] A. Sinha, *Linear Systems: Optimal and Robust Control*, CRC Press, 2007.

[18] S. Bhattacharyya, A. Datta, L. Keel, *Linear Control Theory: Structure, Robustness, and Optimization*, CRC Press, 2009.

[19] S. Nakamori, "New H-infinity tracking control algorithm based on integral equation approach in linear continuous-time systems," *International Journal of Mathematics, Statistics and Operations Research*, vol. 1, no. 2, pp. 109-124, 2021.

[20] J. Gadewadikar, F. Lewis, M. Abu-Khalaf, "Necessary and sufficient conditions for H infinity state output-feedback control," *Journal of Guidance, Control, and Dynamics*, vol. 29, no. 4, pp. 915-920, 2006.

[21] K. Ogata, *Discrete-Time Control System*, 2nd Edition, Prentice Hall, 1995.

[22] S. Baniardalani, "Observer based fault diagnosis systems using continuous-time delay petri nets," *Jordan Journal of Electrical Engineering*, vol. 7, no. 4, pp. 324–343, 2021.

[23] S. Nakamori, "Centralized robust multi-sensor Chandrasekhar-type recursive least-squares Wiener filter in linear discrete-time stochastic systems with uncertain parameters," *Jordan Journal of Electrical Engineering*, vol. 7, no. 3, pp. 289–303, 2021.